

LORA Performance Analysis with Superposed Signal Decoding

Jean Michel de Souza Sant'Ana, *Student Member, IEEE*, Arliones Hoeller, *Member, IEEE*,
Richard Demo Souza, *Senior Member, IEEE*, Hirley Alves, *Member, IEEE*, and
Samuel Montejo-Sánchez, *Member, IEEE*

Abstract—This paper considers the use of successive interference cancellation (SIC) to decode superposed signals in Long Range (LORA) networks. We build over a known stochastic geometry model for LORA networks and include the effect of recovering colliding packets through SIC. We derive closed-form expressions for the successful decoding of packets using SIC taking path loss, fading, noise, and interference into account, while we validate the model by means of Monte Carlo simulations. Results show that SIC-enabled LORA networks improve worst-case reliability by up to 34%. We show that, for at least one test scenario, SIC increases by 159% the number of served users with the same worst-case reliability level.

Keywords—*Internet-of-Things, Stochastic Geometry, Successive Interference Cancellation, LORAWAN.*

I. INTRODUCTION

The Internet-of-Things demands machine-type communications (MTC) to serve massive numbers of devices with low energy consumption and reasonable reliability. The first two requirements are addressed by Low-Power Wide-Area (LPWA) technologies like Long Range Wide Area Network (LORAWAN), SIGFOX, and NB-IoT. However, to achieve large-scale connectivity and low energy consumption, LPWA networks tend to replace complicated channel control by simpler medium access protocols, at the cost of reliability [1].

The LORAWAN protocol stack, which uses Long Range (LORA) as physical layer technology [2], emerges as a promising LPWA network solution. Its openness facilitates and encourages adoption by both researchers and practitioners,

however it may experience decreased reliability with increased numbers of users [3], [4]. As a solution to improve performance, several works exploit diversity relying on independent realizations of the wireless channel. For instance, time diversity is approached in the form of independent [5] or coded [6], [7] message replications for both LORAWAN or general LPWA networks. These approaches have drawbacks. Message replication improves performance at the cost of increased energy consumption and network usage, flooding the network and reducing the number of supported users.

In a different direction, the combination of power-domain non-orthogonal multiple access (NOMA) and successive interference cancellation (SIC) is a key enabler of next generation spectrum-efficient communications [8]. Moreover, LORA features the capture effect, where one out of several simultaneously received signals can be decoded provided that its signal-to-interference ratio (SIR) is sufficiently high, above a given threshold [9]. In this line, Noreen *et al.* [10] exploit this fact and simulate the performance of LORA with SIC to recover the interfering signals, not only the one recovered by the capture effect. Their results show that SIC can increase network performance. Rachkidy *et al.* [11] investigate interference cancellation at the symbol level and propose two algorithms for implementing the technique. Laport-Fauret *et al.* [12] and Xia *et al.* [13] present techniques to decode superposed LORA signals taking advantage from the preamble and chirp characteristics of LORA technology to tune the signals and remove them separately. However, common to [10]–[13] is the lack of closed-form network performance analysis.

In this paper, we consider the effect of a SIC-enabled gateway, able to recover superposed packets when we have one interfering signal, on the performance of a LORA network. An important advantage of this technique is that network servers and end-devices may operate agnostic of SIC at the gateway, while the method does not require any information on network traffic or a feedback link. Also, our work intends to motivate the implementation of practical techniques previously stated that can decode multiple superposed LORA signals. This paper builds over the LORA network stochastic geometry model originally proposed in [3], extending it to account for SIC-based decoding. Then, we provide a new closed-form performance analysis model, which shows that both the number of nodes in coverage and the average reliability can be substantially increased compared to a regular LORA network.

J. M. S. Sant'Ana, A. Hoeller and H. Alves are with the Centre for Wireless Communications, University of Oulu, Finland.

A. Hoeller and R. D. Souza are with the Dept. of Electrical and Electronics Engineering, Federal University of Santa Catarina, Florianópolis, Brazil.

A. Hoeller is also with the Dept. of Telecommunications, Federal Institute for Education, Science, and Technology of Santa Catarina, São José, Brazil.

S. Montejo-Sánchez is with Programa Institucional de Fomento a la I+D+i (PIDi), Universidad Tecnológica Metropolitana, Santiago, Chile.

Corresponding author: Jean.DeSouzaSantana@oulu.fi

This work was partially supported in Brazil by CNPq, PrInt CAPES-UFSC “Automation 4.0”, INESC P&D Brasil (F-LOCO, Energisa, ANEEL PD-00405-1804/2018); in Finland by Academy of Finland, 6Genesis Flagship (Grant 318927), EE-IoT (Grant 319008), and FIREMAN (Grant 326301); in Chile by FONDECYT Postdoctoral (Grant 3170021) and FONDECYT Regular No. 1201893.

©2020 IEEE. Personal use of this material is permitted. Permission from IEEE must be obtained for all other uses, in any current or future media, including reprinting/republishing this material for advertising or promotional purposes, creating new collective works, for resale or redistribution to servers or lists, or reuse of any copyrighted component of this work in other works.

Table I: LORA uplink characteristics: payload of 9 bytes, $B = 125$ kHz, CRC and header mode enabled [9].

SF	Time-on-Air ToA - ms	Bit rate kbps	Sensitivity dbm	SNR threshold q_i - dB	Duty cycle* $p_i \times 10^{-6}$
7	41.22	5.47	-123	-6	45.8
8	72.19	3.12	-126	-9	80.2
9	144.38	1.76	-129	-12	160.4
10	247.81	0.98	-132	-15	275.3
11	495.62	0.54	-134.5	-17.5	550.7
12	991.23	0.29	-137	-20	1101.4

*duty cycle considering ToA and a message generation period of 15 minutes.

II. LORA

LORA is a sub-GHz Chirp Spreading Spectrum (CSS) technology optimized for long-range and low-power transmissions [2]. It uses quasi-orthogonal spreading factors (SF) that increase link budget and the number of virtual channels at the expense of prolonged Time on Air (ToA). Table I presents the relation between SF, ToA, bit rate, and link budget.

LORAWAN is the most used LORA-based protocol stack, with a star topology where end-devices reach one or more gateways through single-hop links. Gateways have IP connections to network servers. LORAWAN controls channel access with ALOHA and exploits SFs to enable concurrent connections in quasi-orthogonal virtual channels. LORAWAN provides many configurations based on SF, which varies from 7 to 12, and bandwidth (B), usually 125 kHz or 250 kHz for uplink.

III. BASELINE SYSTEM MODEL

Following [4], we consider a circular coverage region $\mathcal{V} \subseteq \mathbb{R}^2$ with radius R meters and area $V = \pi R^2$, with \bar{N} end-devices on average deployed uniformly. We split the coverage region into six rings, each using a different SF, assumed to be orthogonal among them, being SF₇ allocated to nodes within the innermost ring, and SF₁₂ to nodes in the outermost ring. Each ring i is bounded by inner (l_{i-1}) and outer (l_i) radii. We assume that the reference¹ node is d_1 meters from the gateway. We model activity in each ring by a homogeneous Poisson Point Process (PPP) Φ_i with intensity $\alpha_i = 2p_i\rho V_i$, $\alpha_i > 0$, where p_i is the duty-cycle of nodes in ring i , $\rho = \frac{\bar{N}}{V}$ is the spatial density, and $V_i = \pi(l_i^2 - l_{i-1}^2)$ is the area of ring i . The average number of devices in ring i is $\bar{N}_i = \rho V_i$. All devices transmit in the uplink at random using ALOHA, with the same bandwidth B and the same fixed transmit power \mathcal{P}_t .

The distance from node k to the gateway at the origin is d_k meters. We model path loss as $g_k = \left(\frac{\lambda}{4\pi d_k}\right)^\eta$, where $\lambda = \frac{c}{f_c}$ is the wavelength, c is the speed of light, f_c is the carrier frequency, and η is the path loss exponent. The model also assumes Rayleigh fading h_k , thus, fading power is exponentially distributed, *i.e.*, $|h_k|^2 \sim \exp(1)$.

If the reference LORA node transmits the signal s_1 , the received signal at the gateway, r_1 , is the sum of the attenuated transmitted signal, interference and noise,

$$r_1 = \sqrt{\mathcal{P}_t g_1} h_1 s_1 + \sum_{k \in \Phi_i} \sqrt{\mathcal{P}_t g_k} h_k s_k + w, \quad (1)$$

¹We use subscript "1" to denote the reference node under analysis.

where k includes the active nodes in the PPP but the reference node, w is additive white Gaussian noise with zero mean and variance σ_w^2 , and i is the ring the node at d_1 belongs to.

A node is in coverage if it is connected to the gateway (probability H_1) and there is no collision (probability Q_1), which considers the SINR according to [14]. A collision takes place when simultaneous transmissions use the same SF, and the signal-to-interference ratio (SIR) is below the threshold γ . Thus, the coverage probability² is [3], [4]

$$C_1 \approx H_1 Q_1. \quad (2)$$

A. Connection Probability

The connection probability H_1 depends on the distance between a node and the gateway. A node is connected if the signal to noise ratio (SNR) at the gateway is above a threshold. The connection probability is $H_1 = \mathbb{P}[\text{SNR} \geq q_i \mid d_1, i]$, where q_i is the SNR reception threshold, from Table I, dependent on SF _{i} . Therefore, as the instantaneous SNR = $\frac{\mathcal{P}_t |h_1|^2 g_1}{\sigma_w^2}$, H_1 is

$$H_1 = \mathbb{P}\left[|h_1|^2 \geq \frac{\sigma_w^2 q_i}{\mathcal{P}_t g_1} \mid d_1\right] = \exp\left(-\frac{\sigma_w^2 q_i}{\mathcal{P}_t g_1}\right). \quad (3)$$

B. Capture Probability

As in [4], we model the SIR as

$$\text{SIR} = \frac{\mathcal{P}_t |h_1|^2 g_1}{\sum_{k \in \Phi_i} \mathcal{P}_t |h_k|^2 g_k} = \frac{|h_1|^2 d_1^{-\eta}}{\sum_{k \in \Phi_i} |h_k|^2 d_k^{-\eta}}. \quad (4)$$

The probability of a successful reception in the presence of interference, considering the capture effect, is

$$Q_1 = \mathbb{P}[\text{SIR} \geq \gamma \mid d_1], \quad (5)$$

where γ is the capture threshold. As detailed in [4], [5], Q_1 is

$$Q_1 = \exp\left\{-\pi \frac{\alpha_i}{V_i} \left[l_i^2 {}_2F_1\left(1, \frac{2}{\eta}; 1 + \frac{2}{\eta}; -\frac{l_i^{-\eta}}{\gamma d_1^\eta}\right) \dots - l_{i-1}^2 {}_2F_1\left(1, \frac{2}{\eta}; 1 + \frac{2}{\eta}; -\frac{l_{i-1}^{-\eta}}{\gamma d_1^\eta}\right)\right]\right\}, \quad (6)$$

where ${}_2F_1(\cdot)$ is the Gauss Hypergeometric function and l_{i-1} and l_i are the boundaries of the SF _{i} ring the node at d_1 is.

IV. COVERAGE PROBABILITY WITH SIC

According to [3], LORA capture probability presents the near-far problem, where transmissions from nodes further away from the receiver are suppressed by transmissions of nodes closer to the gateway due to path loss. Therefore, the further away the node is from the gateway, the less likely it is that it benefits from the capture effect. However, if the receiver can decode the stronger received message from the colliding

²Note that this is a lower bound, since H_1 and Q_1 are dependent due to fading [15]. Moreover, as LORA specifies two different thresholds, for radio sensitivity and the capture effect [16], the independent approach is convenient. Fortunately, this simplified approach allows us to considerably reduce the complexity of the analytical derivations without relevant changes to the results.

messages, by performing SIC it may be able to decode weaker message too. Although, in theory, SIC could be iteratively to decode several colliding messages, it is unlikely to happen unless transmissions are carefully planned to end, like in power-domain NOMA systems [17]. Fortunately, the case where only two simultaneous signals arrive at a gateway is very common in LORA networks, as shown in Section V. Moreover, considering only a single SIC operation reduces the receiver complexity and decoding latency. Therefore, we consider to use SIC in cases where there are two colliding transmissions, trying to recover both messages.

The coverage probability of the signal of interest accounting for SIC becomes³

$$C_1^{\text{SIC}} \approx H_1 Q_1 + H_1 Q_2,$$

where the first term ($H_1 Q_1$) is C_1 as in (2), *i.e.*, the probability that the signal of interest is decoded because it is sufficiently stronger than noise and interference. The second term ($H_1 Q_2$) considers decoding the interfering signal first. Then, we use SIC and decode the signal of interest without interference once it is sufficiently stronger than noise.

In order to derive the second part of (7), first consider $G_j = |h_j|^2 g(d_j) P_t$ as the channel gain of signal j , $j \in \{1, 2\}$ ⁴. Then, we can write the probability H_2 that the signal of interest s_1 and the interfering signal s_2 are in connection (thus sufficiently stronger than noise), given that s_2 can be captured, as

$$\begin{aligned} H_2 &= \mathbb{P} [G_2 \geq q_i \sigma_w^2 \cap G_1 \geq q_i \sigma_w^2 \mid G_2 \geq \gamma G_1, d_1, i] \\ &= \mathbb{P} [G_1 \geq q_i \sigma_w^2 \mid G_2 \geq \gamma G_1, d_1] \approx H_1. \end{aligned} \quad (8)$$

Moreover, the probability that the interfering signal is sufficiently stronger than the reference signal, so that it can be decoded by the capture effect, is

$$\begin{aligned} Q_2 &\stackrel{(a)}{=} \mathbb{P} \left[\frac{G_2}{G_1} \geq \gamma \mid |\Phi_i| = 1, d_1 \right] \\ &\stackrel{(b)}{=} \mathbb{P} \left[|h_2|^2 \geq \frac{\gamma |h_1|^2 d_1^{-\eta}}{D_2^{-\eta}} \mid d_1 \right] \mathbb{P} [|\Phi_i| = 1] \\ &\stackrel{(c)}{=} \mathbb{E}_{D_2} \left[\frac{d_1^\eta}{d_1^\eta + \gamma D_2^\eta} \right] \alpha_i e^{-\alpha_i}, \end{aligned} \quad (9)$$

where in (a) we consider only one interfering node, and in (b) we decondition from the number of interfering nodes. D_2 is a random variable (RV) describing d_2 . In (c) we average over the fading $|h_j|^2 \sim \exp(1)$ and the cardinality $|\Phi|$, which is a Poisson RV of mean α_i and probability density function (PDF) $f_{|\Phi_i|}(k) = \frac{\alpha_i^k e^{-\alpha_i}}{k!}$, where $k=1$ is the number of interferers.

Then, since nodes are distributed in $\mathcal{V} \subseteq \mathbb{R}^2$, $f_D(d) = \frac{2d}{R^2}$, $0 \leq d \leq R$ [18, eq. (3)]. We generalize the ring-based geometry PDF as $f_{D_2}(d_2) = \frac{2d_2}{l_i^2 - l_{i-1}^2}$, $l_{i-1} \leq d_2 \leq l_i$, which

³Since we are mixing a lower bound (considering H_1 , Q_1 and Q_2 to be independent) with the upper bound $H_2 \leq H_1$, we can only say that this is an approximation, which is better seen in Figure 2 and discussed in Section V.

⁴We use subscript “2” to denote the interfering node, when we apply SIC.

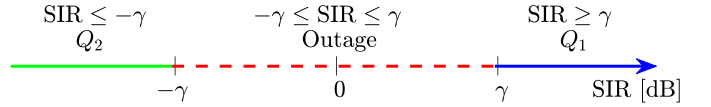


Figure 1: Graphical representation of capture probabilities Q_1 and Q_2 as a function of the SIR of the signal of interest.

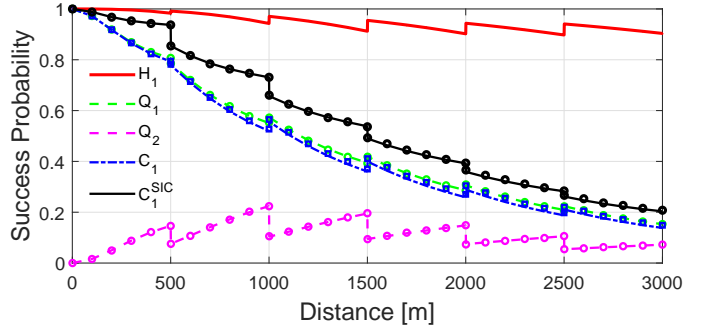


Figure 2: Theoretical (lines) and simulated (markers) probabilities as a function of the distance from the gateway (d_1).

allows us to take the expectation over D_2 and obtain

$$Q_2 = \frac{\alpha_i e^{-\alpha_i} 2d_1^\eta}{l_i^2 - l_{i-1}^2} \int_{l_{i-1}}^{l_i} \frac{x}{d_1^\eta + \gamma x^\eta} dx. \quad (10)$$

Rearranging (10), using the Pochhammer function and the Gaussian Hypergeometric function [19], we have that

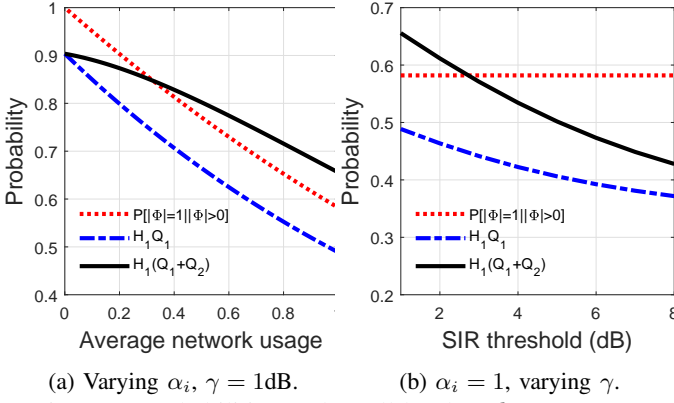
$$\begin{aligned} Q_2 &= \frac{\alpha_i e^{-\alpha_i}}{l_i^2 - l_{i-1}^2} \left[l_i^2 {}_2F_1 \left(1, \frac{2}{\eta}; \frac{2}{\eta} + 1; -\frac{\gamma l_i^\eta}{d_1^\eta} \right) \dots \right. \\ &\quad \left. - l_{i-1}^2 {}_2F_1 \left(1, \frac{2}{\eta}; \frac{2}{\eta} + 1; -\frac{\gamma l_{i-1}^\eta}{d_1^\eta} \right) \right]. \end{aligned} \quad (11)$$

Finally, Q_1 and Q_2 represent probabilities of disjoint events, as illustrated in Figure 1, thus they can not happen simultaneously. When the SIR is above γ , the signal of interest can be decoded due to the capture effect. However, if the SIR is below $-\gamma$, and there is only one interfering signal, it means that this interfering signal SIR is above γ , and thus it can be decoded first, due to the capture effect.

V. NUMERIC RESULTS

We evaluate the impact of SIC in LORA networks in terms of reliability. Unless stated otherwise, we consider $\gamma = 1\text{dB}$, $\eta = 2.8$, $f_c = 868\text{MHz}$, $\mathcal{P}_t = 14\text{dBm}$, $B = 125\text{kHz}$, and $\sigma_w^2 = -174 + F + 10 \log_{10} B = -117\text{dBm}$ with receiver noise figure $F = 6\text{dB}$. Inspired by [3]–[5], we define the deployment area with a fixed radius of $R = 3000\text{m}$, and divide the area in six rings with same width $l_i - l_{i-1} = 500\text{m}$. Nodes in the innermost ring use SF₇, while SF increases with i . Moreover, the duty cycle is $p_i = 1\%$, $\forall i$. This setup configures a typical suburban scenario following European regulations.

In Figure 2 we seek to validate the proposed models by comparing the theoretical expressions to simulations. In the figure, lines represent the expressions in (2), (3), (6), (7), and (11), while marks show the average of 10^5 Monte Carlo simulations considering all dependencies between the events. Note that the



(a) Varying α_i , $\gamma = 1$ dB. (b) $\alpha_i = 1$, varying γ .

Figure 3: Probabilities at the cell border ($d_1 = 3000$ m).

Table II: Number of nodes using the duty-cycles in Table I.

α_i	SF ₇	SF ₈	SF ₉	SF ₁₀	SF ₁₁	SF ₁₂	Total
0.20	2,183	1,247	623	363	182	91	4,689
0.52	5,677	3,241	1,621	944	472	236	12,191
1	10,917	6,233	3,116	1,815	907	454	23,442

approximation in (8) is good as the Monte Carlo simulations of C_1^{SIC} match very well with our proposed framework. For the worst-case scenario in the figure, *i.e.*, for the node at $d_1 = R = 3000$ m, H_1 shows that around 10% of messages are lost due to disconnection, and around 80% are lost due to collisions (Q_1), resulting in coverage probability (C_1) around 13%. However, if SIC for one interfering message is considered, as in this paper, the collision probability drops to around 22% ($Q_1 + Q_2$), resulting in a coverage probability with SIC (C_1^{SIC}) around 20%. Looking to the Q_2 curve, we notice that SIC decoding probability grows with the distance within the SF ring. That is because if the reference signal is closer to the ring outer border, it is likely to be weaker than the interfering signal, what increases the chance of the interfering signal being successfully decoded, thus allowing the reference signal to be decoded too.

Figure 3 considers the performance of the worst-case node in Figure 2, that at the cell border ($d_1 = 3000$ m). Plot 3a shows capture probabilities with and without SIC, *i.e.*, $H_1(Q_1 + Q_2)$ and $H_1 Q_1$, respectively, as a function of network usage rate α_i . Plot 3b shows the same capture probabilities as a function of the SIR threshold γ with fixed $\alpha_i = 1$. In both plots, the dotted/red curve shows $P[|\Phi_i| = 1 | |\Phi_i| > 0]$ – the probability that there is only one interfering signal, provided there is a collision. For instance, when the usage rate is at 100% ($\alpha_i = 1$), 58.2% of the collisions have only one interferer. Plot 3a shows that the gain is significant and increases with network usage, *i.e.*, denser networks benefit more from SIC. Note that in Figure 3a the x-axis is equivalent to varying N_i from 0 to 100 nodes because $N_i = \frac{\alpha_i}{p_i}$ and $p_i = 1\%$, $\forall i$. Plot 3b shows that higher SIR thresholds decrease the SIC benefit, although $H_1 Q_2 = 5.6\%$ for $\gamma = 6$ dB. LORA transceiver manufacturer reports $\gamma = 6$ dB, although recent results show that it can be as low as $\gamma = 1$ dB [4], [20], where $H_1 Q_2 = 16.7\%$.

Since $\alpha_i = 2p_i \rho V_i = 2p_i N_i$ and we fix p_i and V_i , the results in Figure 3a can be extrapolated trading-off duty cycle (p_i) for

number of nodes (N_i). This is shown in Table II considering the ToA and duty cycles from Table I. Results in Table II consider all nodes running the same application. If $\alpha_i = 1$ and $\gamma = 1$, the network would support 23,442 nodes with worst-case packet loss due to interference of 51.1% without SIC and 34.4% with SIC. Moreover, suppose one wants to plan the network for a maximum loss of 20%. From Figure 3a, $H_1 Q_1 > 0.8$ for $\alpha_i < 0.20$ and $H_1(Q_1 + Q_2) > 0.8$ for $\alpha_i < 0.52$. Then, Table II shows that the use of SIC increases the number of nodes from 4,689 to 12,191 ($2.59\times$).

VI. CONCLUSIONS

We proposed a stochastic model extension for LORA networks considering SIC at the gateway, with at most two colliding packets. Such assumption was shown to be representative of most of collision events. The proposed method significantly increases the LORA network performance in terms of coverage probability, while such benefit comes at no cost at the nodes, as the SIC processing is performed only at the gateway. In future work, we aim to maximize the success probability by transmit power allocation that maximizes $Q_1 + Q_2$.

REFERENCES

- [1] W. Ayoub *et al.*, “Internet of mobile things: Overview of LORAWAN, DASH7, and NB-IoT in LPWANs standards and supported mobility,” *IEEE Commun. Surveys Tuts.*, vol. 21, no. 2, Q2 2019.
- [2] LoRAWAN 1.0.3 Specification, LoRA Alliance, Jul. 2018.
- [3] O. Georgiou and U. Raza, “Low power wide area network analysis: Can LoRA scale?” *IEEE Wirel. Commun. Lett.*, vol. 6, no. 2, Apr 2017.
- [4] A. Mahmood *et al.*, “Scalability analysis of a LORA network under imperfect orthogonality,” *IEEE Trans. Ind. Informat.*, vol. 15, no. 3, pp. 1425–1436, Mar 2019.
- [5] A. Hoeller *et al.*, “Analysis and performance optimization of LoRA networks with time and antenna diversity,” *IEEE Access*, vol. 6, 2018.
- [6] P. J. Marcelis *et al.*, “Dare: Data recovery through application layer coding for LoRAWAN,” in *IEEE/ACM IoTDI*, Apr 2017.
- [7] S. Montejo-Sánchez *et al.*, “Coded redundant message transmission schemes for low-power wide area IoT applications,” *IEEE Wireless Commun. Lett.*, vol. 8, no. 2, Apr 2019.
- [8] S. M. R. Islam *et al.*, “Power-domain non-orthogonal multiple access (NOMA) in 5G systems: Potentials and challenges,” *IEEE Commun. Surveys Tuts.*, vol. 19, no. 2, Q2 2017.
- [9] AN120.22 LoRA Modulation Basics, Semtech Corporation, Mar 2015.
- [10] U. Noreen *et al.*, “LoRA-like CSS-based PHY layer, capture effect and serial interference cancellation,” in *24th European Wireless Conf.*, 2018.
- [11] N. E. Rachkidy, A. Guitton, and M. Kaneko, “Decoding superposed LoRA signals,” in *IEEE 43rd Conf. on Local Comput. Netw.*, Oct 2018.
- [12] B. Laporte-Fauret *et al.*, “An enhanced LoRA-like receiver for the simultaneous reception of two interfering signals,” in *PIMRC*, 2019.
- [13] X. Xia *et al.*, “Ftrack: Parallel decoding for LoRA transmissions,” in *Conf. on Embdd. Networked Sensor Syst.*, 2019.
- [14] M. Haenggi, *Stochastic Geometry for Wireless Networks*. USA: Cambridge University Press, 2012.
- [15] J. Lim *et al.*, “Spreading factor allocation for massive connectivity in LoRA systems,” *IEEE Commun. Lett.*, vol. 22, no. 4, 2018.
- [16] SX1272/73 - 860 MHz to 1020 MHz Low Power Long Range Transceiver, Semtech Corporation, Mar 2017.
- [17] O. López *et al.*, “Aggregation and resource scheduling in machine-type communication networks: A stochastic geometry approach,” *IEEE Trans. Wireless Commun.*, vol. 17, no. 7, 2018.

- [18] Z. Bharucha and H. Haas, "The distribution of path losses for uniformly distributed nodes in a circle," *Research Lett. in Commun.*, 2008.
- [19] A. Daalhuis, "Hypergeometric function," in *NIST Handbook of Mathematical Functions*. NY, USA: Cambridge Univ. Press, 2010, ch. 15.
- [20] D. Croce *et al.*, "Impact of LoRA imperfect orthogonality: Analysis of link-level performance," *IEEE Comm. Lett.*, vol. 22, no. 4, 2018.